Indian Journal of Pure & Applied Physics
Vol. 59, October 2021, pp. 693-699

# Growth Kinetics, Optical studies of Pure and $Mg^{2+}$ Doped Nickel Cadmium Oxalate Single Crystals

P S Rohith, N Jagannatha*, K V Pradeepkumar, M S Mangala, K P Nagaraja & Delma D'Souza
PG Department of Physics, FMKMC College, A Constituent College of Mangalore University, Madikeri-571 201, India

*Received 15 January 2020; accepted 22 September 2021*

Growth of pure (nickel cadmium oxalate) and $Mg^{2+}$ doped nickel cadmium oxalate (MNCO) single crystals were grown by the single diffusion gel method at room temperature, by optimizing the various growth parameters such as specific gravity of sodium meta silicate (SMS), gel pH, gel temperature, gel aging, concentration of supernatant solution and concentration of oxalic acid. The morphology and composition of elements present in the crystals were identified using SEM-EDX analysis. The FTIR study shows that the occurrences of C=O, C-O, C-C, O-H and M-O bonding within the crystal lattice. The triclinic crystal system with *P-1* space group were identified using, X-ray diffraction method. The absorbance, transmittance, energy gap, refractive index (n), reflectance (R) and insulating behaviour of the grown crystals were analysed using UV-Visible spectrophotometer.

**Keywords:** Nickel cadmium oxalate, SMS, SEM-EDX, Refractive index, Reflectance

## 1 Introduction

Extensive researches have been carried out over the years on the growth of defect free single crystals due to their wide applications in the field of optoelectronics, linear and non-linear mechanics and solid-state lasers[1, 2]. The crystal growth is a heterogeneous chemical process in which one phase of a compound is converted into another phase. Crystal growth from aqueous solution is known from long time, but control of large nucleation is a problem[3,4]. Gel method is relatively simple and inexpensive. In the present investigation pure and $Mg^{2+}$ doped nickel cadmium oxalate crystals were grown by single test tube gel diffusion method using silica hydro gel as media of growth. The grown crystals were characterized and their morphological and optical properties were measured. The results obtained for $Mg^{2+}$ doped nickel cadmium oxalate (MNCO) crystals were compared with the intrinsic nickel cadmium oxalate (NCO) crystals. The present paper aims to carry out the growth and characterization of NCO and MNCO single crystals in silica gel at ambient temperature. For the preparation of oxalates of metal ions or mixture of metal ions, plenty of publications are concerned. Because of the exceptional chemical and physical properties and also due to the vast applications, alkaline earth elements-based crystals have acquired extensive appreciation in modern years[5,6]. More generally, most of the oxalate crystals exhibit water insolubility, corrosion resistance, insulating behaviour, possesses high leakage resistance and good optical behaviour[7-9]. In view of this, the grown crystals were employed for various characterization techniques.

## 2 Experimental Methods

Single diffusion gel technique was employed to grow NCO and MNCO crystals at ambient temperature. Chemicals used for growing NCO and MNCO crystals were Sodium Meta Silicate (SMS-$Na_2SiO_3.9H_2O$), Oxalic acid ($C_2H_2O_4.2H_2O$), Nickel Chloride ($NiCl_2.6H_2O$), Cadmium Chloride ($CdCl_2.2.5H_2O$) and Magnesium Chloride ($MgCl_2.2H_2O$) of AR grade.

Silica hydro gel was prepared by mixing 0.5 M oxalic acid with desired moles of SMS solution. To control damage and premature gelling, oxalic acid is drop by drop to SMS with constant stirring[10]. Adjusted the pH of the gel between a value of 3.5 and 5 by mixing the oxalic acid and sodium metasilicate in various proportions by volume. The resulted solution (5mL:4mL) was transferred to test tubes with 9 mL each and allowed to set for gelling[11,12]. After setting the gel, 1M nickel chloride and 1M cadmium chloride solutions (2mL: 2mL) poured over the gel surface along the sides of the test tube, without

*Correponding author (Email: jagannathnettar64@gmail.com)

disturbing the gel. $Cd^{2+}$ and $Ni^{2+}$ ions diffuse slowly through the narrow pores of the gel to react with oxalate ions, giving rise to the formation of single crystals of [Ni: Cd]($C_2O_4$). $3H_2O$.

$Mg^{2+}$ doped [Ni: Cd]($C_2O_4$). $3H_2O$ single crystals grown by adding 0.5 M magnesium chloride along with 1M nickel chloride and 1M cadmium chloride solutions (0.2mL: 2mL: 2mL) over the gel surface.

The growth process of NCO and MNCO crystals completed in about 3 weeks. Growth process was optimized and nucleation centres were controlled by varying gel parameters and concentrations of reactant mixtures[11-13]. Experiment was carried out at different specific gravities of SMS (1.030 to 1.060 $g.cm^{-3}$ in steps of 0.02 $g.cm^{-3}$), various concentrations of oxalic acid (0.2 to 1 M in steps of 0.1 M), and concentrations of reactant solution (0.2 to 1 M in steps of 0.1 M).

After harvesting the fully-grown crystals, structural characterization was performed using X-ray powder diffraction technique. XRD patterns were obtained using Minflex 600 Rigaku with CuKα (λ=1.54Å) radiation at a scan speed of 1° $minute^{-1}$. Chemical constituents of the NCO and MNCO crystals were estimated using CARL ZEISS FESEM attached with EDS system (Oxford instruments). Bruker (Alpha) KBr Fourier Transform Infrared Spectrophotometer (FTIR) was used to identify the functional groups associated with the crystals. The spectrum was recorded for the wave number range 400-4500 $cm^{-1}$. Absorbance, transmittance, reflectance and band gap of intrinsic and doped crystals were analysed with the aid of UV-Visible spectrophotometer (UV-1800 Schimadzu) in the spectral range 190-1200 nm.

## 3 Results and Discussion

Table 1 displays a detailed summary of the optimized growth parameters of NCO and MNCO crystals and grown crystals are shown in the Fig. 1.

Table 1 — Optimized growth parameters of NCO and MNCO crystals

| Parameters | Optimum condition | |
|---|---|---|
| | NCO | MNCO |
| Specific gravity ($g.cm^{-3}$) | 1.040 | 1.038 |
| pH of gel | 4.50 | 4.25 |
| Concentration of $CdCl_2$ and $NiCl_2$ | 1M | 1M |
| SMS: Oxalic acid (mL) | 5:4 | 5:4 |
| Gel setting period | 80 h | 95 h |
| Concentration of $MgCl_2$ | -- | 0.5M |
| Period of growth | 3 weeks | 3 weeks |
| Physical appearance | Transparent | Transparent |
| Lattice type | Triclinic | Triclinic |

The fabrication of electronic devices for various applications needs defect free crystals, therefore the interpretation of plastic deformation, morphology of the crystals is important[14,15]. The morphology of the synthesized NCO and MNCO crystals were analyzed by scanning electron microscope shown in Fig. 2. A low magnification SEM images show that the sample consists of many rectangular shapes of nanocrystals. Fig. 3 shows the FESEM images of the as-grown crystals. The valley shaped dislocations are due to the plastic deformation caused by thermal stresses at the nucleation site[16]. Due to the doping of magnesium, the crystal surface becomes fine with well-shaped sharp edges.

The Energy-dispersive X-ray (EDX) spectrum is shown in Fig. 4. The spectrum depicts the occurrences of expected major elements such as Cadmium, Nickel, Magnesium, Carbon, and Oxygen of the title compound. The weight % and atomic weight % of the elements present in the lattice of NCO and MNCO crystals are summarized in Table 2. The EDX result shows the cationic distribution of NCO is $Cd^{2+}$: $Ni^{2+}$ = 4.03: 1, whereas MNCO crystals constituted with cationic distribution, $Cd^{2+}$: $Ni^{2+}$: $Mg^{2+}$= 155.76: 42.24 : 1. EDX analysis clearly reveals the domination of $Cd^{2+}$ and $Ni^{2+}$ ions over the dopant $Mg^{2+}$ ions.

Powder X-ray Diffractogram of NCO and MNCO crystals are shown in Fig. 5. The occurrence of highly resolved intense peaks at specific 2θ values indicates the high crystallinity of the grown material[17]. The observed XRD pattern of the crystals was indexed using the N-TREOR09 program. Cell parameters of grown crystals are given in Table 3. The grain size is determined by measuring the width of the line with

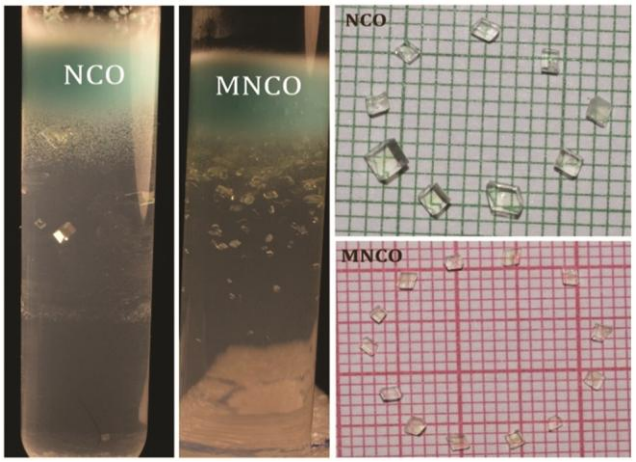


Fig. 1 — Photograph of the grown NCO and MNCO crystals.

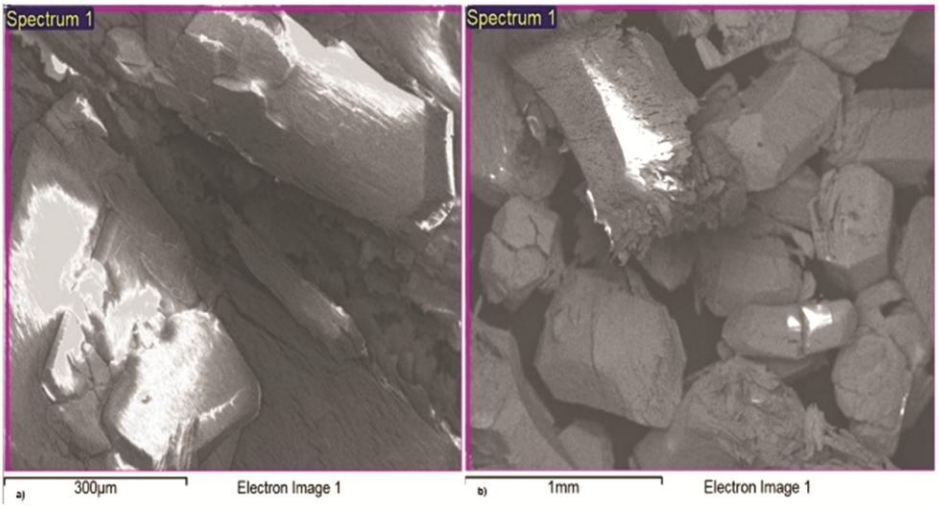


Fig. 2 — SEM images of (a) NCO and (b) MNCO crystals.

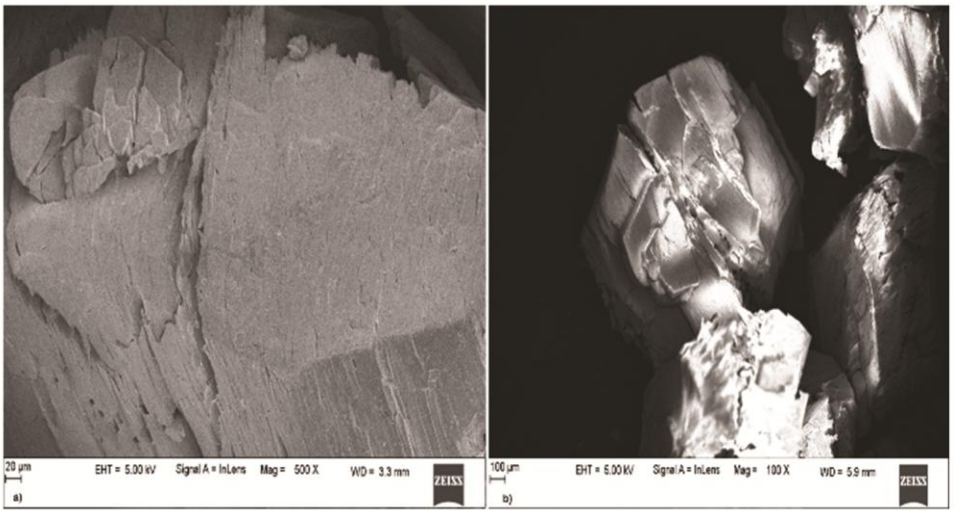


Fig. 3 — FESEM images of (a) NCO and (b) MNCO crystals.

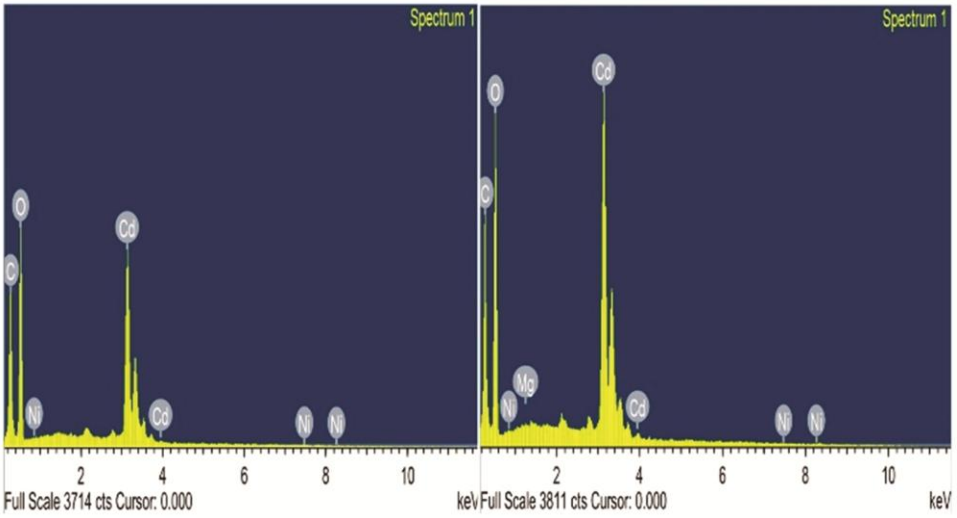


Fig. 4 — EDX spectra of (a) NCO and (b) MNCO crystals.

the highest intensity peak. The crystallite size for the most preferred orientation was evaluated using Debye Scherer formula (1),

$$\text{Grain size, } D = \frac{k\lambda}{\beta \cos\theta} \quad ...(1)$$

Where 'k' is '0.9', 'λ' represents the wavelength of X-rays and 'β' the half-width full maximum of intensity.

FTIR spectra of NCO and MNCO crystals depict the different functional groups, which results in a shift in wave numbers of absorption bands shown in Fig. 6.

Table 2 — EDX data of NCO and MNCO crystals.

| Crystals | Elements | Weight % | Atomic % |
|---|---|---|---|
| NCO | O | 44.72 | 61.59 |
| | Ni | 0.42 | 2.16 |
| | Cd | 38.08 | 5.46 |
| | C | 16.78 | 30.79 |
| | Total | 100.00 | |
| MNCO | Mg | 0.05 | 0.04 |
| | C | 16.08 | 30.54 |
| | O | 42.84 | 61.08 |
| | Cd | 41.02 | 5.33 |
| | Ni | 0.01 | 3.00 |
| | Total | 100.00 | |

Table 3 — Cell parameters of NCO and MNCO crystals.

| Cell parameters | NCO | MNCO |
|---|---|---|
| a (Å) | 5.99 | 5.97 |
| b (Å) | 6.64 | 6.66 |
| c (Å) | 8.46 | 8.45 |
| α° | 74.56 | 74.67 |
| β° | 74.32 | 74.05 |
| γ° | 81.09 | 80.94 |
| Volume (Å$^3$) | 311.07 | 310.80 |
| Space group | P-1 | P-1 |
| Grain size (Å) | 412.01 | 778.58 |

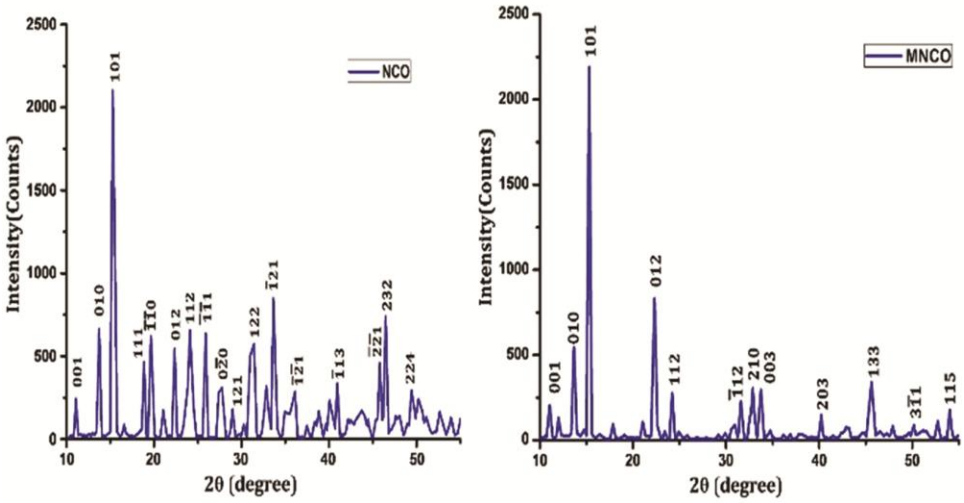


Fig. 5 —Powder X-ray Diffractogram of NCO and MNCO crystals.

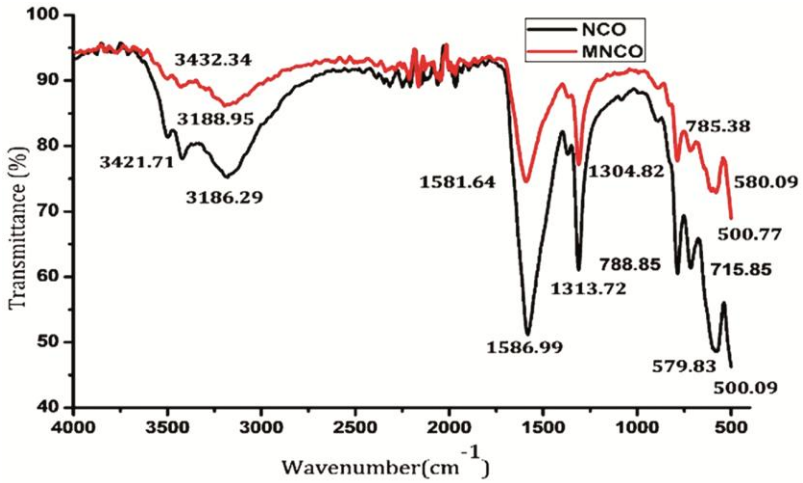


Fig. 6 — FT-IR spectra of (a) NCO and (b) MNCO crystals.

FTIR results of NCO and MNCO crystals were listed in Table 4. Both the crystals showed the presence of intense broad bands around 3500 to 3100 $cm^{-1}$, due to the symmetric and asymmetric stretching of the O-H group which confirms the presence water of crystallization[18,19]. Strong asymmetrical bands around 1580–1600 $cm^{-1}$ are attributed due to the C=O stretching of carboxylate ion[20]. The sharp absorption peaks at 1300–1320 $cm^{-1}$ are due to C-C vibrations and C-O stretching[21]. The absorption bands at 790–710 $cm^{-1}$ are due to O-H out of plane bending and metal-oxygen (M-O) bonding (Metal = Cd, Mg and Ni)[22]. The observed absorption peaks below 700 $cm^{-1}$ correspond to O-M stretching of NCO and MNCO crystals respectively.

Table 4 — FTIR peak assignment of NCO and MNCO crystals

| Peak Assignment | Wavenumber | |
|---|---|---|
| | NCO | MNCO |
| Symmetric and asymmetric stretching of OH group and water of crystallization. | 3421.71 & 3186.29 | 3432.34 & 3188.95 |
| C-O and C-C Stretching | 1586.99 | 1581.64 |
| C=O Stretching, O-H bending | 1313.72 | 1304.84 |
| O-H out of plane bending | 788.85 | 785.38 |
| M-O Stretching | 579.83 & 500.09 | 580.09 & 500.77 |

From the UV transmission spectrum, the lower cut-off wavelength for NCO and MNCO crystals were found to be 240.01 nm and 246.62 nm respectively as shown in Fig. 7 (a). This special characteristic lower cut off peaks at 240.01 and 246.62 nm for NCO and MNCO crystals agreed to the transition (n-$\pi$*) due to a metal-to-ligand (M-O) charge transfer[23,24].

Transmittance spectra shown in Fig. 8, in which MNCO crystals show more transparency than pure NCO crystals in the visible region. Which signifies

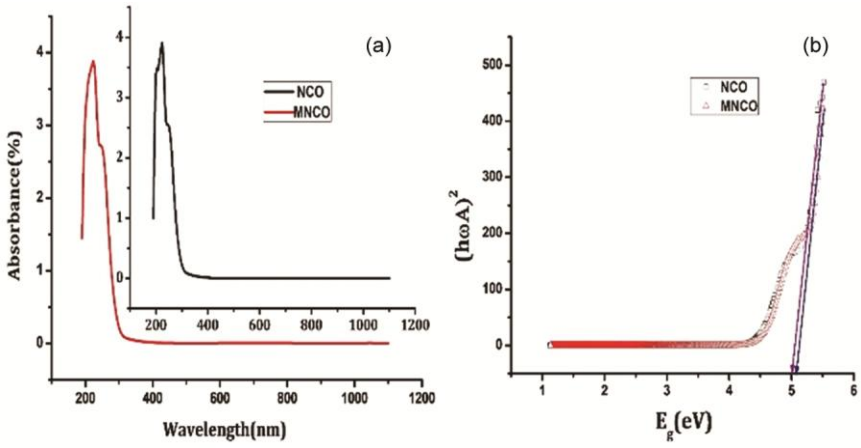


Fig. 7 — a) Absorption spectrum and b) Tauc's Plot of NCO and MNCO crystals.

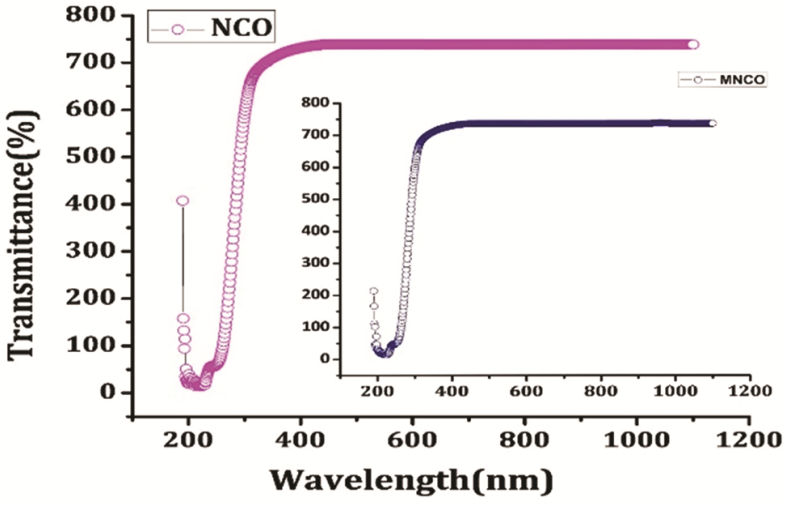


Fig. 8 — UV-Vis transmittance spectrum of NCO and MNCO crystals.

Table 5 — Calculated optical parameters of as grown crystals

| Crystals | Wavelength (nm) | Energy gap (eV) | Ref. Index (n) | Reflectance (R) |
|---|---|---|---|---|
| NCO | 240.01 | 5.17 | 1.95 | 0.103 |
| MNCO | 246.62 | 5.03 | 1.98 | 0.107 |

that the grown crystals can be used as a predominant material for exhibiting optoelectronic device fabricating applications.

The energy dependence of the absorption co-efficient in the high photon energy region is given as

$$\alpha = \frac{2.303}{t} \log \frac{1}{T} \quad ...(2)$$

Where α is the absorbance, 'T' is the transmittance and t is the thickness of the crystal.

The corresponding Tauc's plots[25] are depicted in Fig. 7(b). The optical energy-gap was determined by extrapolating the linear portion of Tauc's plots and is found to be 5.17eV for NCO and 5.03eV for MNCO respectively.

The relation between the refractive index (n) and the energy gap ($E_g$) were given by the expression [26,27].

$$E_g e^n = 36.3 \quad ...(3)$$

This relation is suitable for the energy gap greater than 0 eV. Dispersion is an important property for optical activity of the as-grown samples. Further studies on the refractive index (n) and reflectance (R) of the crystals are calculated by the expression [28].

$$R = \frac{(n-1)^2}{(n+1)^2} \quad ...(4)$$

The calculated band gap energy, high value of refractive index and low value of reflectance from the given Table 5. shows that the as-grown crystals have wide transparency window and more transparency to transmit the light from 250 to 1100 nm. As a result, the title crystals have been shown to be useful material for the nonlinear optical applications[29,30].

## 4 Conclusions

The good quality, defect free single crystals of nickel cadmium oxalate (NCO) and $Mg^{2+}$ doped nickel cadmium oxalate (MNCO) were successfully grown by single diffusion method at ambient temperature (26 ºC). Size and quantity of grown crystals were changed by varying specific gravity of SMS solution, gel age, gel pH and the concentration of upper and lower reactants. EDX spectral studies confirms the presence of expected major elements. The cationic distributions of both the crystals confirms the mixing of cations in pure (NCO) crystal and doping of magnesium into the NCO crystal lattice. FTIR spectrum of NCO and MNCO crystals reveal the presence of water of crystallization, functional and metal-oxygen bonded groups. Existence of high energy-gap in UV visible spectrophotometric studies confirm that the crystal is an insulator suitable material for the fabrication of optoelectronic devices. Higher refractive index and lower reflectance of the crystals support the usefulness of newly fabricated crystals in non-linear optical device applications.

## 5 Acknowledgment

The authors are thankful to the scientific officer DST-PURSE Laboratory Mangalore University, Chairman Department of studies in Physics Mangalore University, Director USIC Mangalore University, Director Innovation Centre MIT Manipal and The Director STIC Cochin for providing facilities for the characterization and technical support to carry out the work.

## References

1 Pradyumnan P P & Shini C, *Indian J Pure Appl Phys*, 47 (2009) 199.
2 Rohith P S, Jagannatha N & Pradeepkumar K V, *J Appl Chem*, 8 (2019) 1838.
3 Jebapriya J C, Jonathan D R & Kiruparvathy S S, *Opt Mater*, 107 (2020) 110035.
4 Vimal G, Mani K P, Gijo Jose, Biju P R & Ittyachen M A, *J Cryst Growth*, 20 (2014) 404.
5 Arora S K, Patel V, Chudasama B & Amin B, *J Cryst Growth*, 275 (2005) 657.
6 Rohith P S, Jagannatha N & Mangala M S, *J Phys Conf Ser*, 1495 (2020) 012005.
7 Sanjeevannanavar M M & Jagannatha N, *AIP Conf Proc*, 2220 (2020) 060009.
8 Patel A R & Venkateswara Rao A, *Bull Mater Sci*, 4 (1982) 527.
9 Jagannatha N & Mohan R P, *Bull Mater Sci*, 16 (1993) 365.
10 Rohith P S & Jagannatha N, *J Mater Environ Sci*, 11 (2020) 788.
11 Sanjeevannanavar M M & Jagannatha N, *AIP Conf Proc*, 2220 **(**2020) 060009.
12 Yadav H, Sinha N & Kumar B, *Mater Res Bull*, 64 (2015) 194.
13 Rohith P S, Jagannatha N & Pradeepkumar K V, *J Appl Chem*, 8 (2018) 1033.
14 Korah I, Joseph C & Ittyachen M A, *J Min Mater Char Eng*, 9 (2010) 1081.
15 Manani N H, Jethva H O & Joshi M J, *IOSR J Appl Phys*, 12 (2020) 25.
16 Khaled Mohammed M, Ibtisan Jasin K & Abdullah H, *J Appl Chem*, 3 (2014) 1036.
17 Pradeepkumar K V & Jagannatha N, *J Appl Chem*, 8 (2019) 1893.

18 Selasteen F D, *Int J Phys*, 2 (2016) 29.
19 Mathivanan V & Haris M, *Pramana J Phys*, 81 (2013) 177.
20 Rohith P S, Jagannatha N & Pradeepkumar K V, *Bull Mater Sci*, 44 (2021) 01.
21 Dharmaprakash S M & Mohan R P, *Bull Mater Sci*, 8 (1986) 511.
22 Rohith P S & Jagannatha N, *Mater Today Proc*, 5 (2019) 85.
23 Sanjeevannanavar M M & Jagannatha N, *AIP Conf Proc*, 2269 (2020) 030008.
24 Daisy Se F & Alfred C R S, *J Cryst Proc Technol*, 6 (2016) 11.
25 Tauc J & Grigorovici V R, *Phys Status Solidi B*, 15 (1966) 627.
26 Reddy R R, Anjaneyulu S, *Phys Status Solidi A*, 174 (1992) 91.
27 Moss T S, *J Phys Stat Sol (B)*, 131 (1985) 415.
28 Rohith P S, Jagannatha N & Pradeepkumar K V, *Int J Chem Tech Res*, 13 (2020) 91.
29 Vasudevan P, Shankar S & Jayaraman D, *Bull Korean Chem Soc*, 34 (2013) 128.
30 Ramachandra Raja C & Gokila G, *Spectrochim Acta Part A*, 72 (2009) 753.